Determination of anisotropic elastic constants of superlattice thin films by resonant-ultrasound spectroscopy

Nobutomo Nakamura,[a] Hirotsugu Ogi, and Masahiko Hirao
Graduate School of Engineering Science, Osaka University, Machikaneyama 1-3, Toyonaka, Osaka 560-8531, Japan

Teruo Ono
Institute for Chemical Research, Kyoto University, Gokasho, Uji, Kyoto 611-0011, Japan

(Received 24 June 2004; accepted 8 October 2004; published online 15 December 2004; corrected 16 December 2004)

Superlattice thin films are expected to show elastic anisotropy because of lattice misfits at interfaces among different elements. This study demonstrates that resonant-ultrasound spectroscopy and laser-Doppler interferometry can determine anisotropic elastic constants of superlattice thin films. Mechanical resonance frequencies of a layered specimen composed of a substrate and deposited thin film depend on the elastic constants, mass densities, and dimensions of the substrate and thin film. X-ray diffraction measurement determines accurately the total thiskness of a multilayer thin film. Therefore, the elastic constants of the multilayer thin film can be derived from measured resonance frequencies, provided that mode identification on observed resonance frequencies is achieved. We measure the resonance frequencies by a piezoelectric tripod and identify the vibration modes by measuring the displacement distributions on the specimen surface using laser-Doppler interferometry. We apply the present method to a Co/Pt multilayer $[\mathrm{Co}(4\ \text{Å})/\mathrm{Pt}(16\ \text{Å})]_{500}$ showing the perpendicular magnetic anisotropy. The in-plane elastic constants are larger than those of bulks by 1%–7%. This is attributed to internal strain due to lattice misfit at the Co–Pt interfaces through interatomic anharmonicity. © *2005 American Institute of Physics*. [DOI: 10.1063/1.1828221]

I. INTRODUCTION

Thin films often show anomalous mechanical, magnetic, optical, and electrical properties. Especially, epitaxially grown multilayer thin films show outstanding properties such as perpendicular magnetic anisotropy (PMA).[1] For these properties, internal elastic strain plays an important role. Noble-metal/magnetic-material multilayers, which show PMA, have lattice misfits as large as 10% at the interfaces. The lattice misfit causes an inconceivably large elastic strain, which would not occur in bulk materials because of dislocation movements. PMA occurs because the large elastic strain could change the magnetization direction from the in-plane direction to the out-of-plane direction, thereby releasing a portion of elastic strain through magnetostriction effect.

Such a large elastic strain should also vary the elastic properties through interatomic anharmonicity. Yang *et al.*[2] reported the "supermodulus" effect in Au/Ni and Cu/Pd multilayers; their elastic constants were significantly larger than those predicted from the elastic constants of constituents. They measured the elastic constants by a bulge-testing method. Baral *et al.*[3] supported Yang *et al.* results by measuring flexural and tensional moduli of Cu/Ni films. However, Davis *et al.*[4] reported that no supermodulus effect appeared in Cu/Pd and Cu/Ni multilayers, which were microscopically the same specimens as those used by Yang *et al.* and Baral *et al.* Cammarata *et al.*[5] also reached a negative result for the elastic enhancement in Cu/Ni multilayer foils with a nanoindentation method. Huang and Spaepen[6] used a tensile test for measuring in-plane Young's modulus of Ag/Cu multilayers and observed no anomaly within the error limit of 30%. Thus, the interpretation has not been settled regarding the elastic constants in multilayer thin films.

We attribute such an inconclusive discussion to two factors. First is the difficulty of making an epitaxially grown multilayer. Before discussing the elastic constants of superlattice, epitaxial interfaces should be studied and confirmed. In order to epitaxially deposit different elements, we have to deposit an element in extremely low pressure carefully controlling depositing layer thickness. In this study we use a molecular-beam-epitaxy (MBE) method to make a superlattice, and confirm the periodicity by a x-ray diffraction (XRD) measurement. Epitaxial bonds at interfaces are confirmed by magnetization measurement using superconducting quantum interference device (SQUID).

The second factor is the difficulty of determining the elastic constants of thin films. Measurements used in the previous studies were highly affected by the gripping effect and accuracy of the film-thickness measurement. Because superlattice multilayers are expected to be elastically anisotropic between the in-plane and out-of-plane directions, they may show transverse isotropy and possess five independent elastic constants, denoted by C_{11}, C_{33}, C_{12}, C_{13}, and C_{44}. (Throughout this study, we use a Cartesian coordinate system, where the x_3 axis is along the out-of-plane direction and the x_1 and x_2 axes lie parallel to the film surface.) However, most of previous studies assumed a multilayer to be isotropic and

[a]Electronic address: nobutomo@me.es.osaka-u.ac.jp

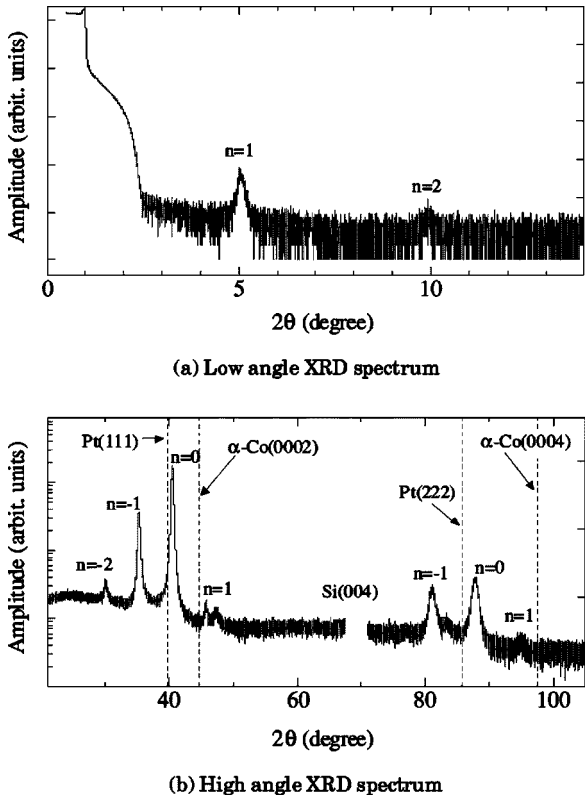

FIG. 1. X-ray diffraction spectra of Co/Pt multilayer deposited on (001) face of monocrystal silicon substrate. Dashed lines indicate predicted XRD angles of bulk Pt and Co.

failed to discuss its elastic anisotropy. Here, we develop an advanced method using resonant-ultrasound spectroscopy (RUS) coupled with laser-Doppler interferometry. It determines inversely the multilayer C_{ij} from free vibration resonance frequencies of the multilayer/substrate specimen. The inverse calculation requires mode identification on the observed resonance frequencies. We achieve this by measuring surface displacement of specimen vibrating at resonance frequency using laser-Doppler interferometer. We apply this RUS/laser method to a Co/Pt multilayer thin film deposited on a Si substrate.

II. MATERIAL

Co/Pt superlattice thin film was prepared by the MBE method on (001) surface of a monocrystal silicon substrate, measuring $5.992\times4.492\times0.208$ mm^3. The pressure before the deposition was 9×10^{-9} Torr and it varied during deposition between $1-9\times10^{-8}$ Torr. The deposition rate was 0.3 Å/s for both of Co and Pt. At first, a 50-Å Pt buffer layer was deposited on the substrate surface. Then, Co and Pt were deposited alternately 500 times. The thickness ratio of the Co and Pt layers was controlled to be 1/4 and modulation wavelength was determined to be 17.7 Å from the XRD satellite-peak angles.[7] The total film thickness was 890 nm. Figure 1 shows the XRD spectra from the Co/Pt multilayer at low-angle and high-angle regions. Satellite peaks appear, which confirm the constant modulation wavelength. Pt (111) and α-Co (0002) peaks would appear between the satellite peaks.

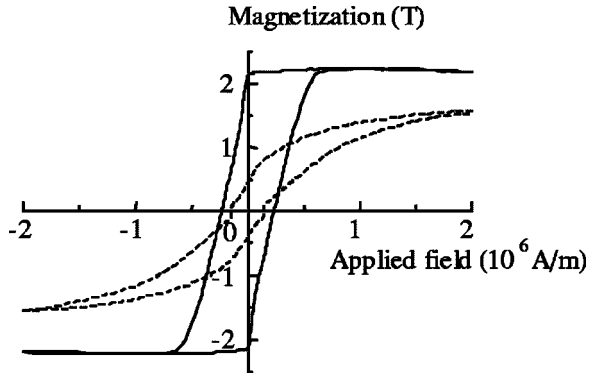

FIG. 2. Magnetic hysteresis loops of Co/Pt superlattice with applied magnetic field parallel to (dashed curve) and perpendicular to (solid curve) the film surface.

Figure 2 shows magnetic hysteresis loops, indicating that the easy axis of magnetization is perpendicular to the film surface. Lin *et al.*[8] reported that the easy axis of the Co/Pt multilayer changed from along the out-of-plane direction to along the in-plane direction as the Pt-layer thickness decreased while the Co-layer thickness was unchanged. As the Pt-layer thickness decreases, the elastic strain in the Pt layer increases and that in the Co layer decreases. This result supports the view that a large elastic strain in the Co layer is indispensable for PMA. Thus, observation of PMA can be a proof for epitaxial bonds at the interfaces.

We assume that the Co/Pt multilayer macroscopically shows transverse isotropy, and the elastic constants are given by

$$[C_{ij}]=\begin{bmatrix} C_{11} & C_{12} & C_{13} & 0 & 0 & 0 \\ C_{12} & C_{11} & C_{13} & 0 & 0 & 0 \\ C_{13} & C_{13} & C_{33} & 0 & 0 & 0 \\ 0 & 0 & 0 & C_{44} & 0 & 0 \\ 0 & 0 & 0 & 0 & C_{44} & 0 \\ 0 & 0 & 0 & 0 & 0 & C_{66} \end{bmatrix}, \tag{1}$$

where $C_{66}=(C_{11}-C_{12})/2$.

III. METHOD

Mechanical free-vibration resonance frequencies of a film/substrate specimen depend on dimensions, mass densities, and all the elastic constants of film and substrate. The dimensions and densities are measurable. The substrate C_{ij} are determined inversely by measuring the resonance frequencies of the substrate alone before the deposition of the film (usual RUS approach).[9,10] The film C_{ij} are then determined by measuring the resonance frequencies of the film/substrate specimen and performing the inverse calculation to find the best fit between the measured and calculated resonance frequencies.[11]

Resonance frequencies of a rectangular parallelepiped are calculated by Lagrangian minimization with Rayleigh–Ritz method.[12,13] Because no analytical solution exists for

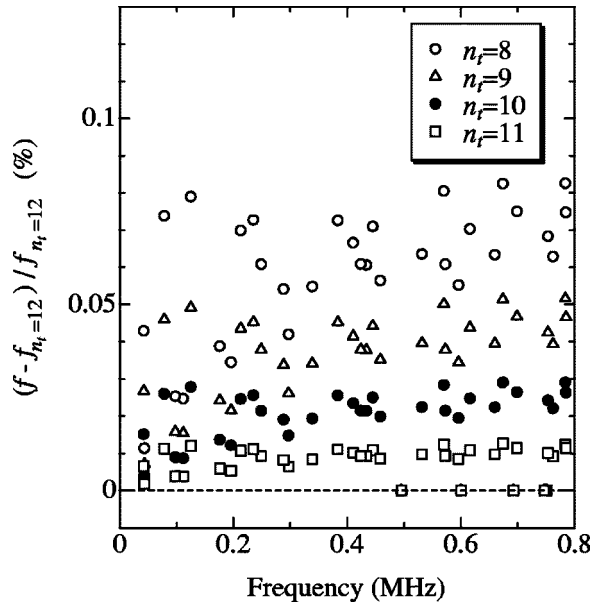

FIG. 3. n_t dependence of calculated resonance frequencies of silicon substrate (n_p=16).

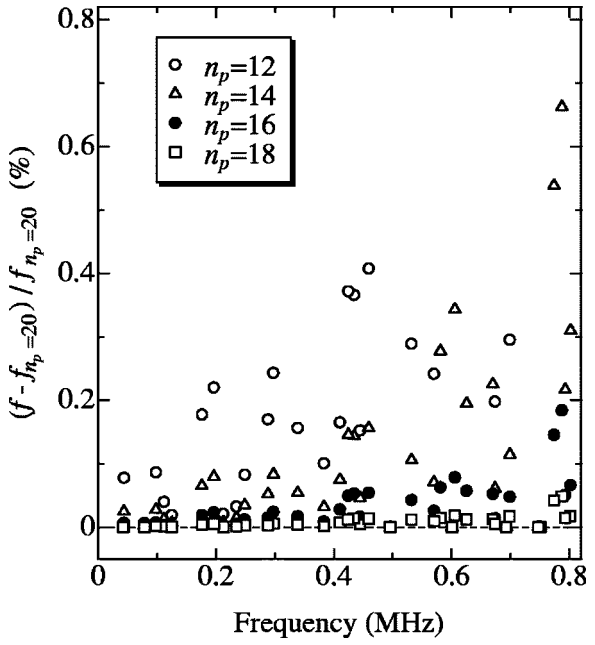

FIG. 4. n_p dependence of calculated resonance frequencies of silicon substrate (n_t=10).

displacements in a rectangular parallelepiped solid subjected to a free vibration, they are approximated by linear combinations of basis functions

$$u_i(x_1,x_2,x_3,t) = \sum_k U_k^i \psi_k^i(x_1,x_2,x_3) e^{j\omega t}. \tag{2}$$

Here, U_k^i denote the expanding coefficients and $\psi_k^i(x_1,x_2,x_3)$ denote basis functions. For a layered parallelepiped specimen, the dependence of the displacement on the x_3 direction must be separated from the others as

$$\psi_k^i(x_1,x_2,x_3) = \eta_m^i(x_3)\zeta_l^i(x_1,x_2), \tag{3}$$

because the displacement gradients become discontinuous at the film/substrate interface with their different moduli. This analysis results in an eigenvalue problem and the resonance frequencies are obtained from eigenvalues of the system ($f = \omega/2\pi$),

$$\omega^2[\mathbf{M}]\{\mathbf{U}\} = [\mathbf{K}]\{\mathbf{U}\}. \tag{4}$$

Here, $[\mathbf{M}]$ denotes the mass matrix associated with the kinetic energy of the system and $[\mathbf{K}]$ denotes the stiffness matrix associated with the strain energy of the system. $\{\mathbf{U}\}$ denotes the eigenvector composed of the expanding coefficients, which provide the displacement distributions in the specimen by Eq. (2). All the independent elastic constants are inversely determined by fitting calculated resonance frequencies to the measurements. Following Heyliger,[14] we use one-dimensional Legendre interpolation polynomials for $\eta_m^i(x_3)$; the total thickness is divided into n_t layers and the displacements are linearly interpolated between the layers. Concerning the in-plane dependence, we use power series $x_1^p x_2^q$ $(p,q=0,1,2,\cdots,)$ for $\zeta_l^i(x_1,x_2)$.

Including higher-order basis functions leads to more accurate frequencies, but takes much longer calculation time. We evaluate dependence of the approximation on the basis-function orders n_t and the order $n_p(=p+q)$. Figures 3 and 4 compare resonance frequencies calculated with various n_t and n_p. When they increase, calculation accuracy improves especially for higher modes. Considering that resonance frequencies observed for the Co/Pt-multilayer specimen were less than 800 kHz, we concluded that n_t=10 and n_p=16 provided the resonance frequencies with enough high accuracy in a reasonable calculation time (10 min with a Pentium 4-2.2 GHz computer).

Because the sensitivity of the thin-film C_{ij} to the resonance frequencies is normally not large, we have to determine the resonance frequencies with accuracy much higher than the calculation accuracy. Previous studies[12,13] sandwiched a specimen between two transducers, which constrained specimen's deformation and changed the resonance frequencies from those of ideal free vibration.[15] We here develop a piezoelectric tripod transducer. It consists of two needlelike transducers and a support needle.[9–11] The specimen is put on the tripod. One transducer is driven by a sinusoidal continuous-wave (cw) signal from a synthesizer and vibrates the specimen with the same frequency as the sinusoidal signal, and the other transducer detects the oscillation amplitude of the specimen. Sweeping the frequency of the cw signal and measuring the oscillation amplitude as a function of frequency, a resonance spectrum is obtained, showing many peaks at the resonance frequencies. Fitting the Lorentzian function around these peaks gives the resonance frequencies. Because the tripod requires neither coupling agent nor external force except for the specimen's weight, it realizes an ideal free oscillation. By measuring the resonance frequencies at a constant temperature $30\pm0.05\,°C$ in vacuum (10^{-3} Torr), reproducibility of measuring the resonance frequencies among independent measurements is better than 10^{-4}, which is smaller by a factor of 100 than the contributions of the film C_{ij} to the resonance frequencies as described below.

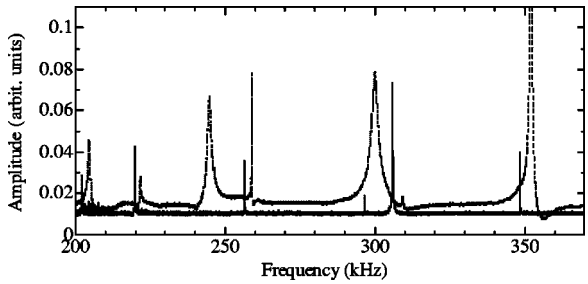

FIG. 5. Resonance spectra of the silicon substrate alone (dashed line) and Co/Pt-multilayer/silicon specimen (solid line).

In the inverse calculation, we must identify measured resonance frequencies. The modes of the calculated resonance frequencies are exactly known, but those of the observed resonance frequencies are unknown. Because mode misidentification leads to physically meaningless elastic constants, correct mode identification is of great importance. We achieve unambiguous mode identification by measuring the surface displacement distribution of the specimen using laser-Doppler interferometry. A laser beam is focused on the specimen surface vibrating at a resonance frequency. The frequency of the reflected laser beam slightly changes depending on the vibration frequency because of the Doppler effect. Scanning the laser beam on the specimen surface draws the two-dimensional distribution of out-of-plane displacement. Equation (2) enables us to calculate the displacement distributions. By comparing the measured and calculated displacement distributions, we make mode identification, leading to the correct elastic constants.

IV. RESULTS

Figure 5 shows resonance spectra observed for the silicon substrate alone and for the Co/Pt-multilayer/silicon specimen. Resonance-peak height and width varied depending on contacting positions between the specimen and needle transducers. Especially, the peak width was highly affected. Thus, the difference of peak widths between before and after the deposition in Fig. 5 does not indicate different internal friction. However, the resonance frequencies were hardly affected by the positions. They decreased after deposition by 1.0–1.5 %. Figure 6 shows an example of measured and calculated surface-displacement distributions of the Co/Pt-multilayer/silicon specimen. Bright regions indicate large amplitudes (antinodes) and dark regions are the nodal lines. The displacement amplitude was less than 1 nm. We see an

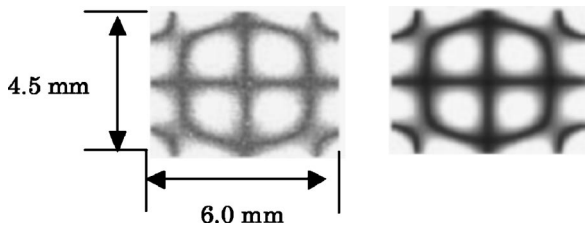

FIG. 6. Measured (left) and calculated (right) displacement-amplitude distributions of Co/Pt-multilayer/silicon specimen at 460.67 kHz.

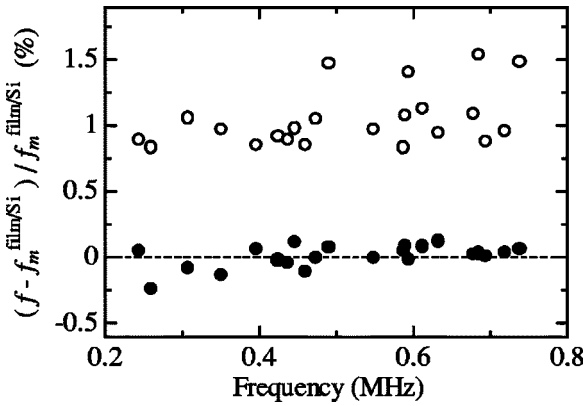

FIG. 7. Comparison between measured and calculated resonance frequencies of Co/Pt-multilayer/silicon specimen (solid circles). Open circles indicate the normalized differences between the resonance frequencies of the Co/Pt-multilayer/silicon specimen and those of the silicon substrate.

excellent agreement between them, which confirms correct mode identification. We identified 22 peaks and entered them in the inverse calculation.

Figure 7 shows differences between measured and calculated resonance frequencies after the convergence. The rms error between them is 0.064%. For comparison, it shows differences between resonance frequencies of the silicon substrate and Co/Pt-multilayer/silicon specimen. They are much larger than the rms error, which indicates that we can deduce the Co/Pt superlattice C_{ij}. We evaluate the measurement accuracy (ΔC_{ij}) from the measurement accuracy of the resonance frequencies (Δf) and sensitivities of elastifc constants to the resonance frequencies ($\partial f / \partial C_{ij}$) as

$$\Delta C_{ij} = \frac{1}{\partial f / \partial C_{ij}} \Delta f. \tag{5}$$

Figure 8 shows normalized sensitivities $(\partial f / \partial C_{ij}) C_{ij} / f$ of the Co/Pt-multilayer C_{ij} to frequencies. Much lower sensitivity

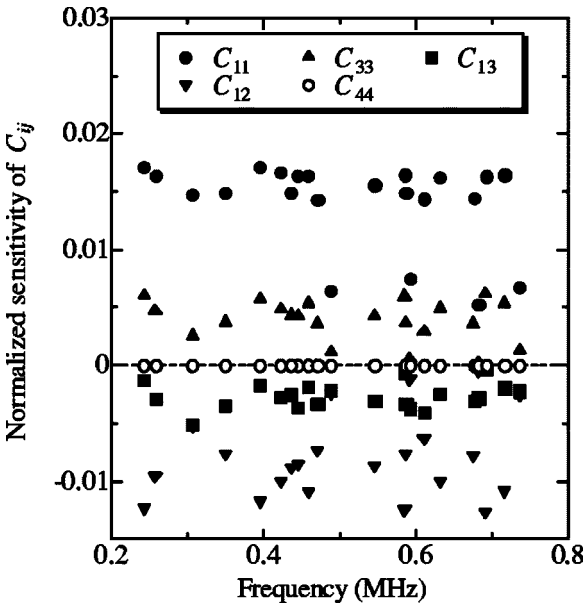

FIG. 8. Normalized sensitivities of Co/Pt-multilayer C_{ij} to the resonance frequencies.

TABLE I. Determined and calculated elastic constants of Co/Pt superlattice, (111)-textured elastic constants of fcc Pt, and elastic constants of hexagonal Co.

	$[Co(4\ Å)/Pt(16\ Å)]_{500}$	Rule of mixture	Pt (111) texture	Co monocrystal Ref. 17
C_{11}	377.9±7.1	360.1	373.6	306.3
C_{33}	367.9±31.5	379.4	384.7	359.4
C_{13}	236.9±10.0	-	231.7	101.9
C_{12}	235.9±46.9	-	242.8	165.1
C_{44}	-	-	56.2	75.3
C_{66}[a]	71.0±2.0	66.4	65.4	70.6
E_1	194.6±4.7	192.9	188.5	210.5

[a]$C_{66}=(C_{11}-C_{12})\lhd 2$.

of the film C_{44} prevents us from determining C_{44} accurately. Table I shows the elastic constant of the Co/Pt multilayer thin film determined in this study. C_{11}, the in-plane Young's modulus E_1, and C_{66} of the multilayer are larger than those predicted from the C_{ij} of the individual bulk materials by 4.9%, 0.9%, and 6.9%, respectively (the detail of predicted values is mentioned below). C_{33} is identical with the predicted value. We see the elastic anisotropy, C_{11}/C_{33}, of a factor 1.02.

V. DISCUSSION

For comparison with determined Co/Pt C_{ij}, we predicted macroscopic Co/Pt C_{ij} from bulk elastic constants of Co and Pt. The XRD measurement indicates that Pt (111) planes are parallel to the film surface. We calculated such a textured C_{ij} by Hill approximation[10] using monocrystal C_{ij}.[16] Because Pt (111) plane is epitaxially bonded with the Co layer, we assumed that [0001] Co plane was perpendicular to the film surface; thus, we used the C_{ij} of α-Co monocrystal[17] whose c plane is parallel to the film surface. We calculated macroscopic elastic constants $C_{11}^{Co/Pt}$, $C_{66}^{Co/Pt}$, $E_1^{Co/Pt}$, and $C_{33}^{Co/Pt}$ of Co/Pt multilayer (Table I) using rule of mixture. Assuming uniform strain field, $C_{11}^{Co/Pt}$, $C_{66}^{Co/Pt}$, and $E_1^{Co/Pt}$ are given with Voigt average.

$$C_{11}^{Co/Pt} = f_{Co}C_{11}^{Co} + f_{Pt}C_{11}^{Pt}, \tag{6}$$

$$C_{66}^{Co/Pt} = f_{Co}C_{66}^{Co} + f_{Pt}C_{66}^{Pt}, \tag{7}$$

$$E_1^{Co/Pt} = f_{Co}E_1^{Co} + f_{Pt}E_1^{Pt}. \tag{8}$$

$C_{33}^{Co/Pt}$ is given by Reuss average.

$$\frac{1}{C_{33}^{Co/Pt}} = \frac{f_{Co}}{C_{33}^{Co}} + \frac{f_{Pt}}{C_{33}^{Pt}}. \tag{9}$$

Here, f_{Co} and f_{Pt} are volume fraction of Co and Pt, respectively. The results are shown in Table I.

Enhancements of the C_{11} and C_{66} are caused by elastic strain at the Co/Pt interfaces. The nearest-neighbored interatomic distance on a Pt (111) plane is larger than that on a α-Co (0001) plane by 10%. Pt layer is compressed and Co layer is extended along in-plane directions. Their completely epitaxial bonds estimate in-plane strains in Pt and Co layers to be -0.024 and 0.080, respectively. An extension of interatomic distance decreases C_{ij} and a contraction increases C_{ij}.[18–20] If the change rate of the C_{ij} caused by the strain was the same in magnitude between extraction and contraction, no change would occur in the macroscopic elastic constants of the multilayer. However, for the same strain, increase of the internal energy by a contraction is significantly larger than that by an extraction because of lattice anharmonicity. Therefore, the observed enhancements of C_{11}, C_{66}, and E_1 are explained by considering the in-plane compression of Pt layer caused by lattice misfit.

VI. CONCLUSIONS

We developed the RUS/laser method to determine the elastic constants of multilayered thin film. The piezoelectric tripod achieved precise measurement of resonance frequencies better than 10^{-4}. We succeeded in correctly identifying all the observed resonance peaks by measuring the displacement distributions on a specimen surface using laser-Doppler interferometry.

We applied our RUS/laser method to Co/Pt multilayer thin film deposited on a silicon substrate. Determined C_{11}, C_{66}, and E_1 are larger than those of bulks by 4.9%, 6.9%, and 0.9%. These enhancements are attributed to compression of the Pt layer, which is caused by lattice misfit at Co/Pt interfaces. Some of determined C_{ij} are larger than those of bulks, however, the significant supermodulus effect as reported in previous studies was not observed.

[1]P. F. Carcia, J. Appl. Phys. **63**, 5066 (1988).
[2]W. M. C. Yang, T. Tsakalakos, and J. E. Hilliard, J. Appl. Phys. **48**, 876 (1977).
[3]D. Baral, J. B. Ketterson, and J. E. Hilliard, J. Appl. Phys. **57**, 1076 (1985).
[4]B. M. Davis, D. N. Seidman, A. Moreau, J. B. Ketterson, J. Mattson, and M. Grimsditch, Phys. Rev. B **43**, 9304 (1991).
[5]R. C. Cammarata, T. E. Schlesinger, C. Kim, S. B. Qadri, and A. S. Edelstein, Appl. Phys. Lett. **56**, 1862 (1990).
[6]H. Huang and F. Spaepen, Acta Mater. **48**, 3261 (2000).
[7]S. S. Jiang, A. Hu, H. Chen, W. Liu, Y. X. Zhang, Y. Qiu, and D. Feng, J. Appl. Phys. **66**, 5258 (1989).
[8]C. J. Lin, G. L. Gorman, C. H. Lee, R. F. C. Farrow, E. E. Marinero, H. V. Do, H. Notarys, and C. J. Chien, J. Magn. Magn. Mater. **93**, 194 (1991).
[9]H. Ogi, N. Nakamura, K. Sato, M. Hirao, and S. Uda, IEEE Trans. Ultrason. Ferroelectr. Freq. Control **50**, 553 (2003).
[10]N. Nakamura, H. Ogi, T. Ichitsubo, M. Hirao, N. Tatsumi, T. Imai, and H. Nakahata, J. Appl. Phys. **94**, 6405 (2003).
[11]N. Nakamura, H. Ogi, and M. Hirao, Acta Mater. **52**, 765 (2004).
[12]I. Ohno, J. Phys. Earth **24**, 355 (1976).
[13]A. Migliori, J. L. Sarrao, W. M. Visscher, T. M. Bell, M. Lei, Z. Fisk, and R. G. Leisure, Physica B **183**, 1 (1993).
[14]P. Heyliger, J. Acoust. Soc. Am. **107**, 1235 (2000).

[15]H. Ogi, H. Ledbetter, S. Kim, and M. Hirao, J. Acoust. Soc. Am. **106**, 660 (1999).
[16]R. E. Macfarlane, J. A. Rayne, and C. K. Jones, Phys. Lett. **18**, 91 (1965).
[17]E. S. Fisher and D. Dever, Trans. Metall. Soc. AIME **239**, 48 (1967).
[18]C. Y. Pao, W. Sachse, and H. Fukuoka, *Physical Acoustics*, edited by W. P. Mason and R. N. Thurston, (Academic, New York, 1984).
[19]Y. Hiki and A. V. Granato, Phys. Rev. **144**, 411 (1966).
[20]H. Ogi, N. Suzuki, and M. Hirao, Metall. Mater. Trans. A **29A**, 2987 (1998).